Effect of Boric Acid on Volatile Fission Products in Conditions Simulating a Severe Nuclear Accident

Citation for the original published paper (version of record):
Börjesson Sandén, F., Pasi, A., Kärkelä, T. et al (2025). Effect of Boric Acid on Volatile Fission Products in Conditions Simulating a Severe Nuclear Accident. Nuclear Technology, In Press. http://dx.doi.org/10.1080/00295450.2025.2462490

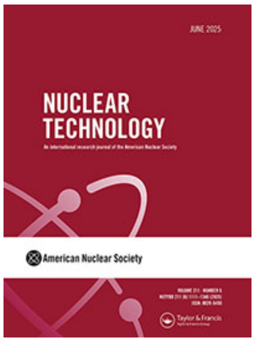

Nuclear Technology

ISSN: (Print) (Online) Journal homepage: www.tandfonline.com/journals/unct20

Effect of Boric Acid on Volatile Fission Products in Conditions Simulating a Severe Nuclear Accident

Fredrik Börjesson Sandén, Anna-Elina Pasi, Teemu Kärkelä, Tuula Kajolinna & Christian Ekberg

To cite this article: Fredrik Börjesson Sandén, Anna-Elina Pasi, Teemu Kärkelä, Tuula Kajolinna & Christian Ekberg (24 Apr 2025): Effect of Boric Acid on Volatile Fission Products in Conditions Simulating a Severe Nuclear Accident, Nuclear Technology, DOI: 10.1080/00295450.2025.2462490

To link to this article: https://doi.org/10.1080/00295450.2025.2462490

NUCLEAR TECHNOLOGY

DOI: https://doi.org/10.1080/00295450.2025.2462490

Effect of Boric Acid on Volatile Fission Products in Conditions Simulating a Severe Nuclear Accident

Fredrik Börjesson Sandén,[a]* Anna-Elina Pasi,[b] Teemu Kärkelä,[b] Tuula Kajolinna,[b] and Christian Ekberg[a]

[a]*Chalmers University of Technology, Kemivägen 4, SE-412 96 Gothenburg, Sweden*
[b]*VTT Technical Research Centre of Finland Ltd, P.O. Box 1000, FI-02044 VTT, Espoo, Finland*

Received November 13, 2024
Accepted for Publication January 20, 2025

Abstract — *Boric acid is expected to play a role in severe nuclear accident chemistry, raising questions about of how it affects the volatile fission products iodine, cesium, and tellurium. Since tellurium and iodine are radiologically related (^{132}Te decays into ^{132}I/^{132m}I with a half-life of 3.17 days) interactions between them are always possible in a severe accident scenario, but research focusing on their interactions is surprisingly scant.*

Experiments were undertaken at the VTT Technical Research Center of Finland using a setup involving the volatilization of tellurium, the injection of iodine as a gas, and boric acid and/or CsI dissolved in water and injected with the help of an atomizer. Analysis of the results included measurements with inductively coupled plasma mass spectrometry (ICP-MS), scanning electron microscopy (SEM) and X-ray photoelectron spectroscopy (XPS).

The results indicate that the volatility of tellurium is significantly increased if tellurium, iodine (I_2), and boric acid are all present together, which was observed through a heightened concentration of tellurium in the liquid trap following such experiments. Furthermore, the formation of tellurium iodide is possible, as determined by SEM-Energy-dispersive X-ray spectroscopy (SEM-EDS) and supported by XPS. These results imply that studies of tellurium in combination with other relevant species should be continued. There is evidence that their volatility can be affected by one another, but the research into this type of interaction is scant.

Keywords — *Volatile fission products, tellurium, iodine, boric acid, severe accident.*

Note — *Some figures may be in color only in the electronic version.*

I. INTRODUCTION

Nuclear accidents differ from most other industrial accidents since they can result in radioactive releases. This happened in the Three Mile Island nuclear accident,[1,2] the Chernobyl accident,[3,4] and the Fukushima-Daiichi accident.[5,6] Especially, volatile fission products can feasibly escape the reactor containment after an accident and be released to the environment. The volatile fission products are noble gases, iodine, cesium, and tellurium.[7] Iodine is especially notorious, as it accumulates in the thyroid gland, and radioactive iodine thus is concentrated and the exposure is prolonged, potentially leading to cancer-related diseases long after the accident and exposure,[8] whereas ^{137}Cs makes radioactive contamination an issue that can last for decades due to its long half-life.

Fission products can form chemical compounds with one another or surrounding material. These compounds exhibit different chemical, physical, and biological

---

*E-mail: sandenf@chalmers.se

characteristics, all of which affect the release of radioactivity. Investigations into the chemistry of volatile fission products is a way to predict and help mitigate the damage they can do to humans and to the environment in the case of a severe nuclear accident.

The most widely used nuclear reactor is the pressurized water reactor (PWR). To control its reactivity, and as part of the emergency shutdown sequence, boric acid is injected into the primary circuit. Natural boron contains about 20% of the isotope ^{10}B, a thermal neutron absorber. Its presence decreases the number of thermal neutrons available for interaction with fissile ^{235}U, thus decreasing reactor power. Boric acid, therefore, is a common chemical in nuclear reactor installations, and it is likely that it, or compounds derived from it, will be present in the case of an accident. If so, its interaction with the volatile fission products should be studied.

Iodine and cesium, and the interactions between them, have been relatively well studied in the context of severe accidents. Some isotopes of particular interest are listed in Table I. Especially, iodine is a concern, as it contributed to a large part of the activity released after both the Chernobyl and the Fukushima accidents.[9,10] The most important isotope, ^{131}I, has a half-life of about 8 days, and thus will decay to a negligible level in about 3 months. The decay of relevant iodine isotopes gives rise to various xenon nuclides, which are chemically inert.

Iodine melts at a temperature of 113.5°C and boils at 184°C at standard pressure. The transport of iodine in severe accidents is rather unique, as it may be transported both as aerosol particles[11] and as gaseous I_2.[12] Aside from the noble gases, other volatile fission products typically are transported as aerosols.[12]

The most important cesium isotopes are listed in Table I. Cesium melts at 28.5°C and boils at 671°C. The volatility and long half-life of ^{137}Cs makes this isotope a radio hazard with ramifications reaching far into the future.

Tellurium is yet another volatile fission product. It is a metalloid that melts at 450°C and boils at 990°C. It has a complex chemistry and can adopt several oxidation states, with the most common being −II, +II, +IV, and +VI. Tellurium dioxide, TeO_2, is a species of note because of its higher melting and boiling points compared to metallic tellurium, 732°C and 1245°C, respectively. The oxidation of tellurium, therefore, in principle decreases its volatility. However, as with many oxides, the volatility may increase in the presence of water vapor[13] through reaction (1),

$$TeO_2(s) + H_2O(g) \rightleftharpoons TeO(OH)_2(g) \quad . \tag{1}$$

From a radio-hazard perspective, tellurium is not as long lasting as cesium (as seen in Table I), as the half-life of the most important tellurium isotope is 3.2 days. This is primarily a short- to medium-term concern. However, during the Chernobyl accident, the activity of released ^{132}Te was one of the highest for individual isotopes, and it was indeed higher than the activities of both ^{137}Cs and ^{134}Cs.[14] Tellurium-132 decays into iodine-132, which has a half-life of roughly 2.3 h.[15] This means tellurium and iodine will coexist, and interactions between them warrants study. Furthermore, the release of tellurium results in a delayed release of iodine, which has implications for the iodine source term.

Tellurium, in its role as a fission product, has been studied before, for instance, in its interaction with the zircalloy cladding,[17] investigations into the potential

TABLE I

Comparison of Releases Between the Chernobyl Accident and the Fukushima-Daiichi Accident for Selected Cs, I, and Te Isotopes*

Nuclide	Half-Life[15]	Decay Product	Estimated Released Activity Chernobyl[16] (PBq)	Estimated Released Activity Fukushima-Daiichi[10] (PBq)
^{129m}Te	33.6 days	^{129}I	240	15
^{132}Te	3.17 days	^{132}I/^{132m}I	1000	180
^{131}I	8.03 days	^{131}Xe/^{131m}Xe	1200 to 1700	150
^{133}I	20.83 h	^{133}Xe/^{133m}Xe	2500	146
^{134}Cs	2.07 years	^{134}Ba	44 to 48	11.8
^{136}Cs	13.16 days	^{136}Ba	36	2.2 to 2.6
^{137}Cs	30.08 years	^{137}Ba/^{137m}Ba	74 to 85	12

*In all releases of the volatile fission products, the Chernobyl accident was significantly worse. Note that there have been several studies of these releases, and that different studies report different releases.

formation of organic tellurides,[18,19] and its role in the reactor sump.[20] Iodine is the most studied fission product, having been the subject of several large-scale studies, including PHEBÚS[21] and VERCORS,[22,23] to name a few.

However, studies specifically on the interaction between tellurium and iodine are surprisingly scarce given that they are radiologically related. As tellurium will never be present without iodine, there will be potential for them to interact. This study aims to investigate the interaction between tellurium and two significant chemical forms of iodine, I_2 and CsI, while also continuing the investigation started in Ref. [24] to further investigate the effects of boric acid on this system.

This paper aims to investigate the effects of boric acid on systems including iodine (both in its elemental form and as cesium iodide) and tellurium, simulating the conditions of a severe nuclear accident. The investigation of all these elements together is a novel concept that requires further study. Specifically, any effects of the volatility of the fission products due to the inclusion of boric acid is of interest.

II. THEORY AND BACKGROUND

II.A. Boron Chemistry

Boron can be used as a means of reactor control due to the high nuclear cross section of the B^{10} nuclide with thermal neutrons. In PWRs, boron is an additive, where it is dissolved in the primary circuit water, often in the form of orthoboric acid (henceforth, referred to as just boric acid). This affects the neutron economy in the reactor, allowing for an alternate method of controlling the reactor aside from the control rods.[25,26]

These uses make boron a likely component of the sump water in a severe accident. However, it should be noted that as boric acid is present as an additive in the PWR primary circuit, its potential for interaction with fission products is not limited to the containment but may potentially also happen in the pressure vessel or the steam generator tubes. This, in turn, makes the relevant temperature range large, from thousands of degrees in the reactor core, to less than 100°C in the containment.

The concentration of boric acid in the reactor varies with the freshness of the fuel, with fresh fuel being more reactive, and thus necessitating a higher concentration of boric acid. As the fuel is consumed, the concentration is lowered. Typical values across a fuel cycle vary between 1 g/l and a few milligrams at the end of the cycle.[25] Relatively concentrated acid (2200 ppm) can also be injected into the circuit as part of an emergency shutdown, meaning that the concentration in the sump during or after a severe accident is likely even higher than that.

Boric acid is not stable at elevated temperatures, but undergoes a series of dehydration reactions, as described in reactions (2), (3), and (4),[27]

$$B(OH)_3 \leftrightharpoons HBO_2 + H_2O, T\sim142°C \ , \tag{2}$$

$$\mathrm{B(OH)_3} \leftrightharpoons \mathrm{HBO_2 + H_2O, T}\sim142°\mathrm{C} \ , \tag{3}$$

$$\mathrm{H_2B_4O_7} \rightleftharpoons \mathrm{2B_2O_3 + H_2O,\ \ T}\sim327^o\mathrm{C} \ . \tag{4}$$

This, however, implies the heating of the pure substance, rather than it being dissolved. Nevertheless, calculations performed with the NucleaToolbox and the database shows that vaporization of boric acid in Ar/H_2O forms $B_3O_6H_3$, and a calculation with FactSage 5.5 indicated gaseous release of $B_3O_3H_3$ between 127°C to 727°C.[28]

However, just as with tellurium, the presence of water vapor affects the volatility of boric oxide. Even at relatively low temperatures (100°C to 300°C), gaseous boron hydroxides can be observed[29] to form from solid B_2O_3. The species is implied to be HBO_2, implying a form of reversal of the combined reactions (3) and (4), summarized as reaction (5),

$$\mathrm{H_2B_4O_7} \leftrightharpoons \mathrm{2B_2O_3 + H_2O, T}\sim327°\mathrm{C} \ . \tag{5}$$

This reaction, of course, is dependent on the temperature and the vapor pressure of the water.

The chemistry and physical characteristics of fission products have been investigated in projects such as VERCORS and PHÉBUS, and in smaller projects aimed at more specific questions. Furthermore, the data gained from the Chernobyl and Fukushima-Daiichi accidents themselves have also provided insight, especially in the relative releases of the different fission products.

II.B. Interactions Between Cesium, Iodine, Boron, and Tellurium

Iodine and cesium have both been relatively well investigated, both in their interactions between one another as well as with boric acid.

According to NUREG-1465, as much as 95% of the iodine that enters the containment from the reactor coolant system will be in the form of CsI.[30] If available, this species will react with molybdenum trioxide, forming cesium molybdates and gaseous iodine. This reaction is also affected by the partial pressure of oxygen in the system. The higher the oxygen partial pressure, the more gaseous iodine is formed.[31] This is postulated to be linked to the oxidation state of molybdenum, as the formation of I_2 only seems to happen when molybdenum is oxidized beyond oxidation state IV+ (beyond MoO_2).[32]

Similar results have been seen for the CsI− boric acid system, where the reactions described in reactions (6) and (7) describe the resulting formation of gaseous iodine and cesium borates,[28]

$$CsI(c) + B(OH)_3(g) \leftrightharpoons CsBO_2(c) + HI(g) + H_2O \tag{6}$$

$$CsI(c) + B(OH)_3(g) \leftrightharpoons CsBO_2(c) + HI(g) + H_2O \ , \tag{7}$$

where (c) indicates a condensed state.

The process described by reactions (6) and (7) has been shown to be very efficient at converting CsI into gaseous iodine. When vaporizing only CsI in inert argon gas with steam, only about 1% of the iodine found was in a gaseous form. Upon the addition of boric acid, 94% of the iodine was in gaseous form.[28] Furthermore, the efficiency of this conversion was affected by the flow rate of the carrier gas, with a high flow rate lowering the conversion.

Similarly, in the presence of water, reactions (8) and (9) are possibilities that further influence the cesium and iodine chemistry,

$$CsI + H_2O \leftrightharpoons CsOH + HI \tag{8}$$

$$CsOH + B(OH)_3 \leftrightharpoons CsBO_2 + 2H_2O \ , \tag{9}$$

where reaction (9), if it happens, consumes CsOH, thus driving reaction (8) farther to the right. Equilibrium calculations indicate that the overall reaction of the reactions (8) and (9) becomes highly relevant at 1027°C, whereas for 727°C, the iodine will largely be present as CsI still, with only 18% being in the form of HI. This nevertheless implies that the presence of boric acid potentially can alter the speciation of iodine and cesium drastically,[33] all depending on the temperature and conditions.

Compared to cesium and iodine, tellurium has been less studied, and its interactions with the other fission products have been less rigorously investigated. It is released from the fuel at a similar time as cesium, so the CsTe-species may be formed in the reactor core during an accident. Examples would include Cs_2Te or Cs_2TeO_3.[34] The stability of these species in atmospheric conditions is uncertain, however, and their formation would be contested by species such as SnTe or even TeO_2, depending on the conditions. Tellurium and cesium did behave in a similar way after the Fukushima-Daiichi accident in that they tended to appear together in aerosols.[35] However, the ratio between them varied significantly.

Tellurium and iodine can react to tellurium iodides. This class of compounds encompasses various ratios between tellurium and iodine, and what compound is formed will depend on the circumstances, as can be seen in the phase diagram presented in Fig. 1. Note that the phase diagram only assumes two solid tellurium iodides, TeI and TeI_4, as it is assumed that these are the only compounds formed in the solid state.[36] However, in the vapor phase, TeI_2 is also formed through the decomposition of TeI_4 to TeI_2 and I_2. This is expected at

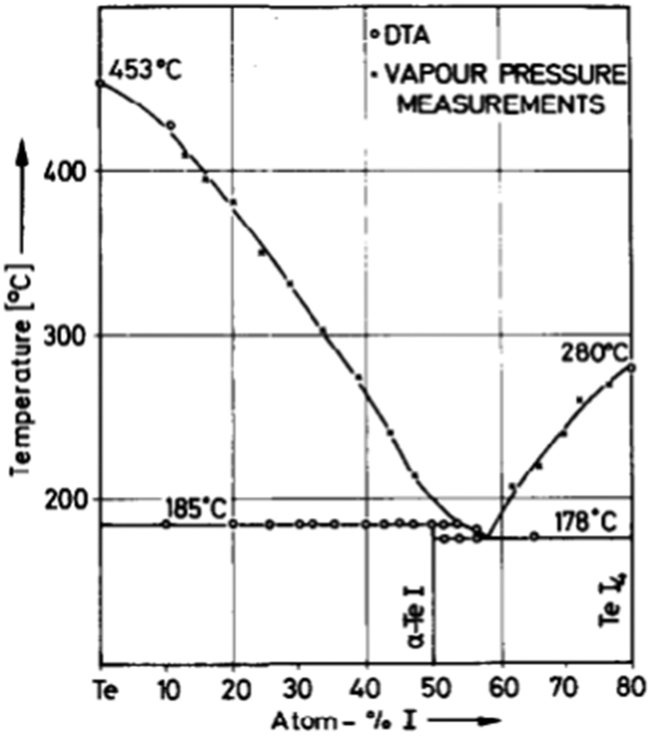

Fig. 1. Phase diagram of the Te-I system[37] (used with permission from the publisher).

temperatures above 500°C, with further decomposition to the basic elements at temperatures above 600°C.[36]

Tellurium iodides have been studied in the context of nuclear reactor technology before by investigating the volatility of iodide in a tellurium matrix,[38] though this research was not directly connected to accident chemistry. The samples investigated were produced by irradiating tellurium metal with neutrons, generating ^{131}I by decay from ^{131}Te. The ratio between the two elements, therefore, was in the range of 10^{10} atoms of Te per atom of I. Still, the results imply that tellurium (sub)iodides do form and remain volatile until temperatures of about 150°C to 200°C. This was determined by allowing the gaseous tellurium iodides to be carried down a furnace with a gradually decreasing temperature.

The interaction between boron and tellurium has been very scarcely reported in the context of severe nuclear accidents. Tellurium and boron are sometimes investigated together in the context of engineering glasses,[39] but this does not answer the questions regarding their behavior in severe accident conditions, which is the focus and novelty of this paper.

III. METHODOLOGY

A total of nine experiments were conducted at VTT in Espoo, Finland, as presented in Table II. An analysis of the samples produced was then conducted in part at VTT and in part at Chalmers University of Technology in Gothenburg, Sweden. The experiments, in principle, were performed in a progressively more complex chemical environment, allowing for the experiments to act as reference points to one another. They can also be considered a further development of the system investigated in Ref. [24].

The temperature in all these experiments was 650°C to simulate the temperature in the primary circuit during a loss-of-coolant accident. The three atmospheres used encompassed both oxidizing and reducing conditions, both of which are theoretically possible during an accident, as well as an inert atmosphere.

Throughout all nine experiments, only singlets were performed, meaning uncertainties were impossible to determine.

III.A. Description of the Experimental Setup Using Iodine Gas

The experiments were performed using two different setups. One setup was used to conduct experiments X.1 and X.2 (X.1, X.2, or X.3 indicates the respective experiment, as seen in Table II), whereas the final experiment for each atmosphere, X.3, which involved CsI, necessitated a slightly different setup. However, both setups drew inspiration from the setup previously used in the cooperation between VTT and Chalmers. Details can be found in Ref. [31], and the system used for the present study is schematically depicted in Fig. 2. The three carrier gases consisted of synthetic air (21% O_2, 79% N_2) for the oxidizing conditions, N_2 for the inert conditions, and 5% H_2 by volume in argon for the reducing conditions.

Two tubular flow furnaces (Entech Vecstar, VCTF 4) were connected in sequence with tubes made from stainless steel (AiSI 316L). These furnaces held the same temperature throughout the experiments and were the only points in the setup where the temperature was measured. The first furnace was loaded with a crucible of Al_2O_3 filled with 5 g of Te (metal, Sigma-Aldrich, purity ≥99.997%) before each experiment. The temperature of this furnace was set to 540°C. The gas flow through this furnace was in total 3 l/min for all three conditions. All the flows in use were controlled by mass flow control units (Brooks S5851, Brooks® Instrument).

TABLE II

Experimental Conditions Investigated Throughout This Work

Experiment	Atmosphere	Injected Through Atomizer	Fission Products
1.1	Oxidizing (air)	–	I, Te
1.2	Oxidizing (air)	$B(OH)_3(aq)$	I, Te
1.3	Oxidizing (air)	$B(OH)_3(aq)$, CsI (aq)	Te
2.1	Reducing (Ar/H_2)	–	I, Te
2.2	Reducing (Ar/H_2)	$B(OH)_3(aq)$	I, Te
2.3	Reducing (Ar/H_2)	$B(OH)_3(aq)$, CsI (aq)	Te
3.1	Inert (N_2)	–	I, Te
3.2	Inert (N_2)	$B(OH)_3(aq)$	I, Te
3.3	Inert (N_2)	$B(OH)_3(aq)$, CsI (aq)	Te

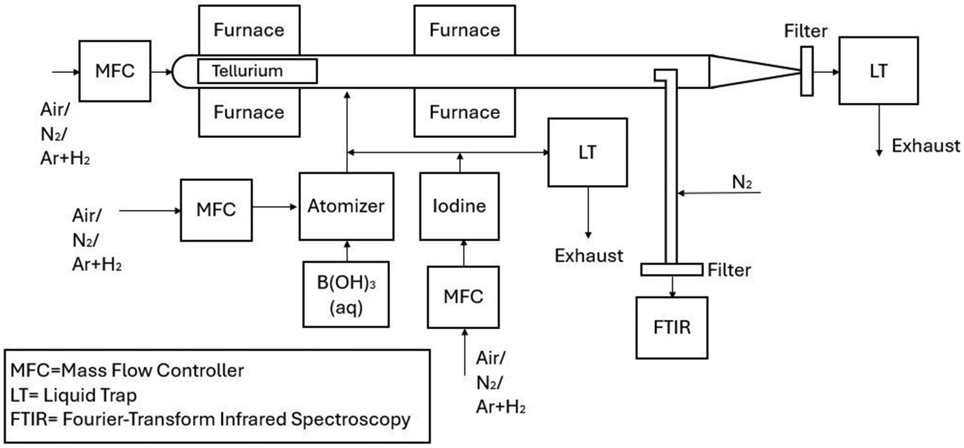

Fig. 2. Schematic depiction of the experimental setup used for most of the experiments.

Between the two furnaces there was a connection where both iodine and boric acid could be introduced to the system. Iodine was supplied by placing pebbles of solid iodine in a sealed bottle, which in turn was heated in a water bath set to 65°C. The flow through the iodine feed was 2 l/min, but before the flow entered the main line, 0.8 l/min was diverted through a liquid trap (100 ml 0.1 M NaOH) and sent to the exhaust. By analyzing the contents of the liquid trap, it was possible to determine the amount of iodine fed during the experiment.

An atomizer fed a solution of 0.2 M boric acid through this middle connection. The atomizer had a flow of 3 l/min. To ensure the total flow through the main line was similar for all conditions, whether or not boric acid was used, another line bypassed the atomizer and delivered a 3 l/min flow in the experiments that does not involve the boric acid solution.

Beyond the junction, another furnace and tube were placed, identical to the first ones. The flow through this furnace contained all species in use for the experiment being run, and added up to a total of 7.2 l/min. The temperature in this furnace was constant across all experiments and set to 650°C.

Finally, beyond this furnace, 2.2 l/min of the flow was diverted to a secondary line, which allowed for an online Fourier transformed infrared spectroscopy (FTIR) measurement during the experiment. Before the FTIR, a filter (MilliPore, MitexTM PTFE, pore size 5 μm) was placed to catch any particulate matter.

The remaining 5 l/min of the flow was sent directly through an identical filter, after which it was diverted through a liquid trap (100 ml 0.1 M NaOH) to catch any species capable of penetrating the filter, especially volatile species. The outlet of the liquid trap was sent to the exhaust.

The first two experiments, X.1 and X.2, for each atmosphere run with this setup were all performed in an uninterrupted sequence. Each condition was run for 30 min. After 30 min, the gas flow after the second furnace was redirected to the exhaust while the filters and liquid traps were changed. This took about 10 to 15 min, after which the next experiment could be started by starting or stopping the relevant gas flows without the need for the furnaces to cool down.

III.B. Description of the Experimental Setup Using Cesium Iodide

To accommodate the use of CsI in the system, the setup had to be modified. This setup is schematically depicted in Fig. 3. These three conditions (experiments 1.3, 2.3, and 3.3) were run in order of reducing, inert, and oxidizing conditions. Each condition followed upon the other, and each condition lasted for 30 min. The method used has been described previously.[31] This means that 3 l/min carrier gas was added through the tellurium furnace and 3 l/min was added through the atomizer introducing $B(OH)_3$. To this liquid (200 ml 0.2 M $B(OH)_3$), 2 g of CsI was added (for a concentration of 38.5 mM). Thus, CsI was added to the system via the same avenue as the $B(OH)_3$ after the tellurium had been volatized but before the reaction furnace at 650°C. Like the previous setup, 2.2 l/min of the flow was diverted to FTIR, whereas the remaining 5 l/min was directed through the filter and the liquid trap. For the experiments with CsI, no iodine vapor was used.

Both of the filters were weighed with a bench scale to the precision of .10 mg before and after the experiments to determine how much material was collected on them.

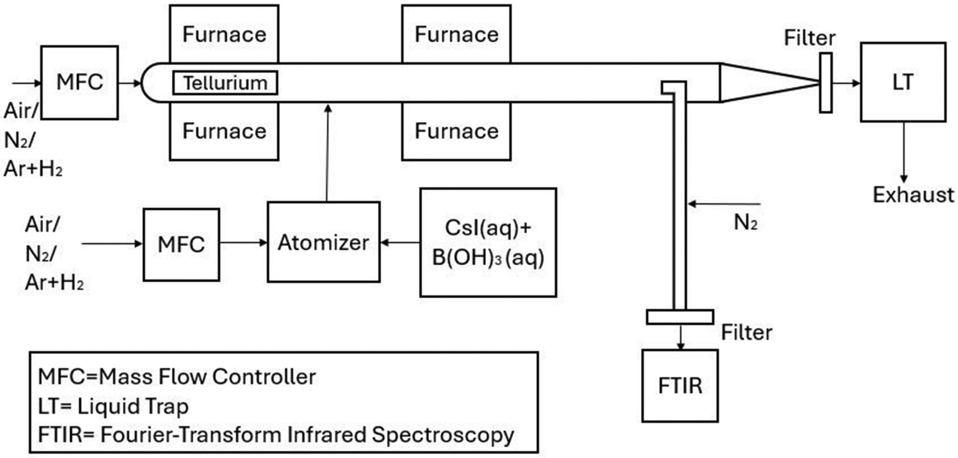

Fig. 3. Schematic depiction of the experimental setup used for the experiments involving CsI.

III.C. Inductively Coupled Plasma Mass Spectroscopy

The liquid traps were analyzed with inductively coupled plasma mass spectroscopy (ICP-MS) (element 2, ThermoScientific) after the experiments to determine the concentration of Te, I, B, and/or Cs. The detection limits for tellurium (Te^{126}) were 0.006 ppb. The samples are diluted with 0.5 M of HNO_3 (Suprapure) before the measurements, and 1 ppb Rh was used as an internal standard. The iodine samples were diluted with 0.1 M of NaOH.

III.D. X-ray Photoelectron Spectroscopy

X-ray photoelectron spectrometry (XPS) was conducted at Chalmers University of Technology, using the PHI5000 VersaProbe III–Scanning XPS Microprobe™ machine. The X-ray source was a monochromatic AlKα source (1486 eV). The beam width was 100 µm, 25 W 15 kV, full-width at half-maximum was 0.654 eV, determined from the $3d_{5/2}$ peak after measuring a sputter-cleaned Ag sample. The system was aligned with Au (83.96 eV), Ag (368.21 eV), and Cu (932.62 eV), and the narrow scan measurements were aligned with the C1s signal at 284.6 eV before analysis. For XPS, the limit of detection depends on the element in question and the sample matrix.[40] However, all expected elements could be determined for this study.

The survey scan proceeded from 0 to 1100 eV with a step size of 1 eV, and the narrow scans had a step size of 0.1 eV. For the C1s signal, the step size was 0.05 eV.

III.E. Scanning Electron Microscopy– Energy-Dispersive X-ray

The filter samples were investigated with scanning electron microscopy (SEM) using the Quanta 200 FEG ESEM (manufactured by FEI) at the Chalmers material analysis laboratory (CMAL). Imaging was based on backscattered electrons and used a 15-kV voltage and a current at about 100 µA.

III.F. Production of Tellurium Iodide

Samples of tellurium iodide were prepared using the stoichiometric ratio of 2 mol of iodine per 1 mol of tellurium. The pure elements were mixed in an evacuated quartz ampule and heated to 400°C. At this point, the substance in the ampoule had melted into a solid lump, well below the melting point of tellurium at 449.5°C. Note that TeI_2 did not exist in the solid phase.[36]

IV. RESULTS

IV.A. Chemical Content of the Liquid Traps

The chemical content of the liquid traps for each experimental condition for tellurium, boron, iodine, and cesium are detailed in Table III. These contents represent the gas-phase species in each condition.

The most trapped species was most often iodine, followed by boron, with tellurium being the species with the lowest concentration in the liquid trap. This held for every experiment, and was not surprising given that iodine gas effectively penetrates the filter to the liquid trap, given that it should occur as a gaseous species. Compared to filter weights (see Sec. IV.C), it seems that the iodine tended to decrease as the number of particles increased, implying that there was a reaction between the particles and the iodine. The iodine content is plotted in Fig. 4.

TABLE III

Contents of the Liquid Traps for the Different Experiments

Experiment	Iodine Content (mM)	Boron Content (mM)	Tellurium Content (µM)	Cesium Content
1.1	5.67	0.46	0.27	–
1.2	6.02	2.26	7.44	–
1.3	0.19	0.34	2.35	Below detection limit
2.1	4.18	0.53	3.21	–
2.2	5.00	1.36	61.28	–
2.3	0.001	0.85	4.70	Below detection limit
3.1	1.30	0.25	0.04	–
3.2	5.28	2.29	117.12	–
3.3	0.13	0.92	5.49	Below detection limit

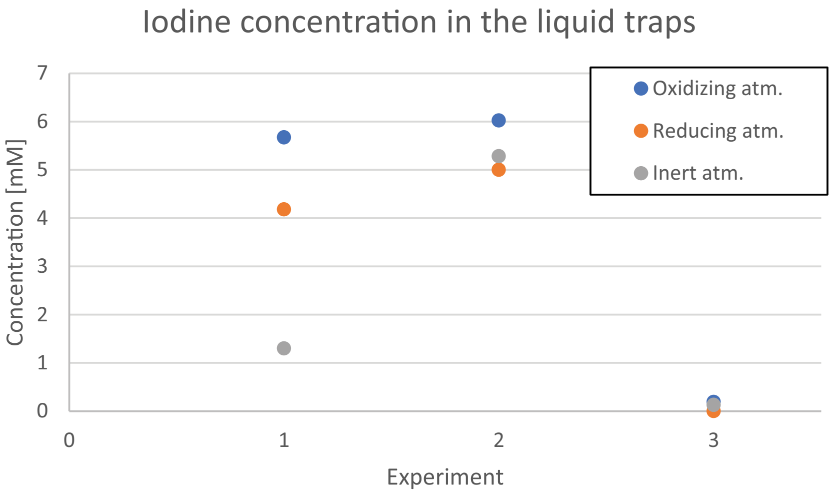

Fig. 4. Iodine concentration in the respective liquid traps. Experiment refers to the different experiments 1, 2, and 3, as labeled in Table II.

Likewise, boric acid is volatile at these temperatures, though it tends to decompose to B_2O_3, which has a negligible vapor pressure even at significantly higher temperatures.[41] However, its interaction with water ought to cause the formation of volatile HBO_2.[29] Volatile derivatives of boric acid have also been seen together with CsI previously.[28] No boric acid was added in the X.1 series of experiments, but the boron content was still consistently present in the liquid trap. This was due to contamination from the borosilicate glass used for the liquid trap. The trap solution was 0.1 M of NaOH, which does etch glass.

Tellurium only had a few volatile species under these conditions, aside from TeH_2, which would only be relevant in reducing conditions (experiments 2.1, 2.2, and 2.3), and was still not very stable as the temperature fell from 650°C.

There was a sharp increase in the tellurium and boron concentrations in the liquid trap in all X.2 experiments compared to X.1. The difference between these was the addition of boric acid, which explains the boron increase. The reason for the tellurium increase is uncertain, but speculation is possible upon considering the interaction between tellurium and iodine, as well as the behavior of boron in the presence of water vapor.

The system including only tellurium and dissolved boric acid in nearly identical conditions (similar setup, same temperature, same carrier gases etc.) has been investigated before.[24] However, no large increase in tellurium concentration could then be observed in the trap, other than for the reducing conditions at 650°C, in which case the increase could be attributed to the formation of TeH_2, which does not explain the increases presented here. Furthermore, since the increase presented here was present for all three atmospheres, its mechanism should be somewhat independent of the atmosphere. The hypothesis for the mechanism behind this increase in volatility is presented in Sec. IV.F.

For the experiments using tellurium, CsI, and boric acid, there were few trends compared to earlier experiments. The tellurium content was in the same order of magnitude across all three atmospheres and generally low. Iodine likewise does not seem to be transported as a volatile species in these conditions, as evidenced by the iodine content being one or two magnitudes lower in these experiments compared to all other conditions. Cesium was never detected in the liquid traps. The boron content, finally, was comparable to all other conditions.

IV.B. Summary of the FTIR Analysis

The FTIR spectra failed to determine any volatile compounds with certainty. Presumably, any volatile species were present in too low of a concentration to determine with FTIR. The limit of detection of the instrument was 1 ppm. This would include TeH_2, which would be expected in some of the experiments performed in reducing conditions. Indeed, in a previous study, TeH_2 was also inferred from the liquid samples, but could still not be determined in the FTIR analysis.[24]

IV.C. Filter Mass Analysis

The filters were weighed to the precision of .10 mg before and after each experiment. The change in the filter weights can be seen in Fig. 5.

Across the range of filters, there is one general remark to be made: The oxidizing atmosphere, no matter the other constituents of the system, makes for the least depositions on the filters. Largely, the low mass can be explained by the oxidation of the tellurium in the crucible into TeO_2, which is not volatile at these temperatures (the crucible was placed before the inlet of the boric acid solution, so there was no increase in volatility due to the presence of water in the crucible). However, the filter from experiments 1.1 (involving iodine, and tellurium) and 1.3 (involving cesium iodine, tellurium, and boric acid) did display for an oxidizing system, a high filter weight, though not as high as in the cases of the reducing or inert atmospheres.

Looking at the corresponding XPS spectra for these two filters (see Sec. IV.E), the main element is tellurium. The signal for tellurium was made up of four different binding energies across the two experiments. For experiment 1.1 they were 576.4 eV and 577.9 eV, and for 1.3, they were 575.7 eV and 576.9 eV. This means three, or potentially four, tellurium compounds may exist in these samples. Comparison to the reference spectra for tellurium compounds suggests that the signals for 576.4 eV and 576.9 eV both belong to a tellurium oxide, either TeO_2 or TeO_3. The signal for 577.9 eV is less certain, but could be attributed either to TeO_3 or the hydrated form $Te(OH)_6$. All these compounds are possible in an oxidized system.

In the case of experiment 1.1, the reason for the large deposition on the filter could be due to a high availability of fresh, unoxidized tellurium in the precursor early in the experiment, contributing to a high deposition on the filter, which was subsequently oxidized. The increased volatility for experiment 1.3 might be linked to the final signal at 575.7 eV. The nature of this signal is uncertain and will be discussed further in Sec. IV.C, which is dedicated to the XPS measurements.

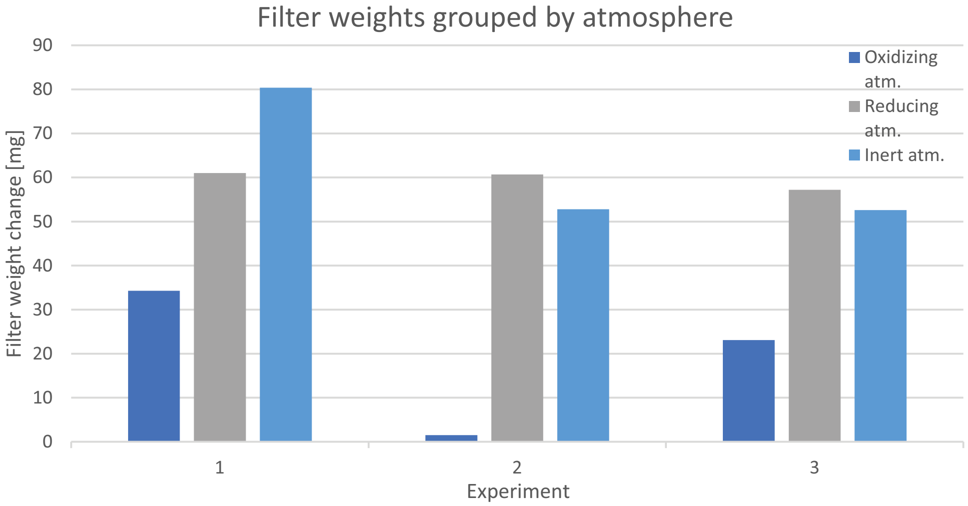

Fig. 5. Increase in filter weight after the different experiments: (1) I + Te, (2) I + Te + $B(OH)_3$, and (3) CsI + Te + $B(OH)_3$.

The reducing experiments all gave a very similar filter mass change after each experiment, implying that there was little change in the volatility of tellurium in either of these conditions. These are also the conditions where tellurium iodides were discovered (see Secs. IV.D and IV.E).

The mass of the filters for the various inert cases was mostly comparable to the reducing conditions, though no tellurium iodide was discovered on these filters. Note that the experiment with the very highest filter weight corresponded to the very lowest content of tellurium in the liquid trap.

IV.D. SEM Analysis of the Filters

A representative SEM micrograph of the filters exposed to the reducing atmosphere (experiment 2.2) can be seen in Fig. 6. The energy-dispersive spectroscopy (EDS) spectra for two representative spots (spot 1 and 2 in Fig. 6) can be seen in Figs. 7 and 8. The crystalline structures seen in Fig. 6 appear to be composed of tellurium iodide. The ratio appears to be roughly equal, implying TeI as the species. The iodine appears to be collected in these crystals, as no EDS measurements other than those performed on the crystals showed any iodine. The porous material appears to only contain tellurium.

A representative SEM micrograph of the filters exposed to inert atmosphere (experiment 3.2) can be seen in Fig. 9. The filter exposed to inert atmosphere contained only very few, significantly smaller crystals; mostly the surface was uniformly composed of tellurium, as determined by the EDS spectrum seen in Fig. 10.

The lack of iodine deposition, and its prevalence in reducing conditions, implied that the formation of tellurium iodide was tied to the reducing atmosphere. A possibility is that the hydrogen telluride reacted with the iodine to form TeI_2. Another possibility is the formation of hydrogen iodide as an intermediary, and the direct reaction between molecular iodine and hydrogen was used industrially to produce HI. However, it then requires a palladium catalyst,[41] which was not present in this study.

The tellurium aerosols were similar in all cases, consisting of submicron, spherical particles. This description and the size line up with what was discovered when investigating the effect of boric acid on just tellurium.[24] According to the XPS analysis of these particles, they were also mostly tellurium, and the size was similar to what can be seen in the micrographs in Figs. 6 and 9. This could be expected, as these spherical aerosols seem to consist of almost pure tellurium, which was also seen in the study without iodine.[24] It appears that the presence of iodine did not change the aerosol formation very much, aside from the presence of tellurium iodide in some cases.

For the oxidizing atmosphere, the deposited particles were strongly oxidized, and the electrical conductivity was poor. No conclusions could be drawn from those images.

IV.E. XPS Analysis of Filters

For each of the experiments, a survey spectrum from the particle deposition on each filter was collected to get

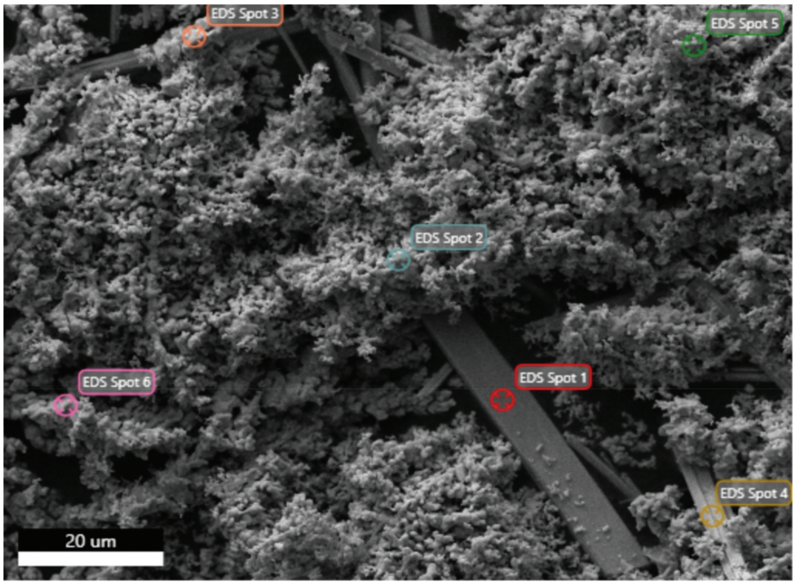

Fig. 6. SEM micrograph of the filter exposed to Te, I, $B(OH)_3$, and reducing atmosphere. Notice the large crystals embedded among the porous coverage.

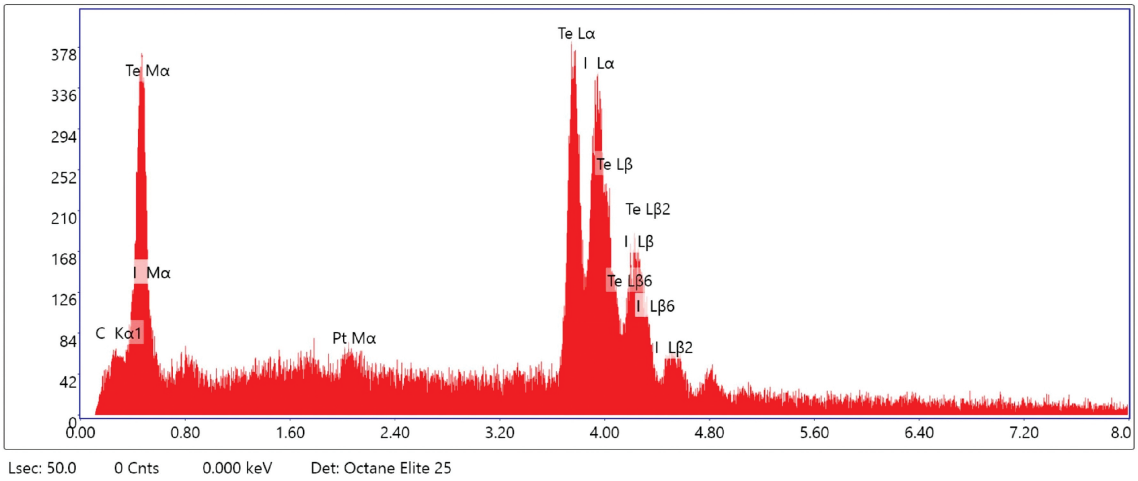

Fig. 7. EDS spectrum of spot 1 in Fig. 6, the large crystal. The crystal surface seems to be composed of tellurium iodide, and quantification states the elements are present in roughly equal amounts.

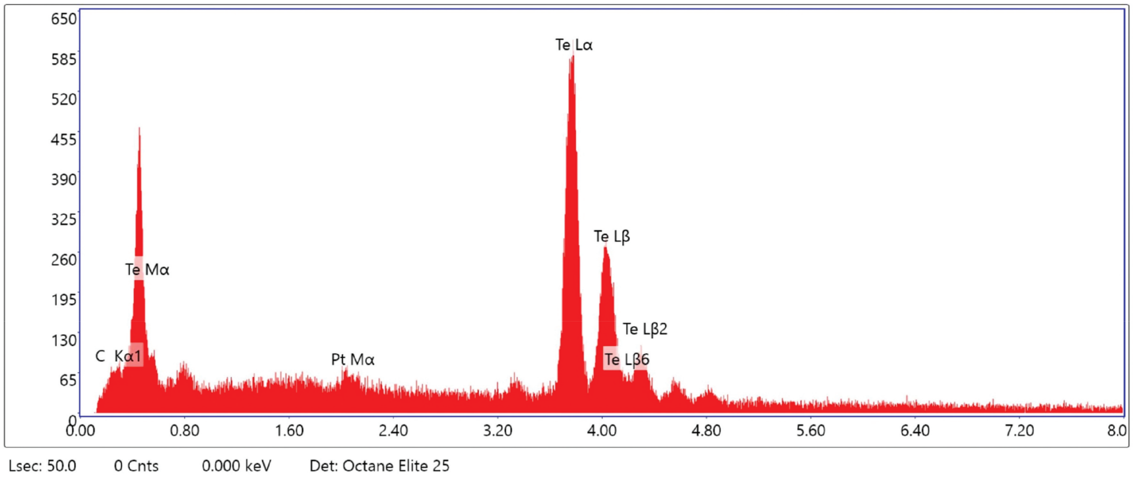

Fig. 8. EDS-spectrum of spot 2 in Fig. 6, the porous coverage. The porous coverage seems to be composed of practically pure tellurium metal. There is no indication of iodine in this spectrum.

an idea of the relative surface abundances of the different elements. Furthermore, the signal of each individual element was investigated with a finer resolution to determine chemical shifts exhibited by each element, which in turn, helped with identification of the chemical state of the elements. The signal peak(s) for each element and each experimental condition are summarized in Table IV.

There were also spectra for the boron content in the conditions where boron was relevant, but in general, the signal was very weak and difficult to interpret with certainty. The literature seems to suggest transport mainly as boric acid or the trimer of metaboric acid ($H_3B_3O_6$) in temperatures between 127°C and 727°C.[28]

For the tellurium speciation, there were four to five broad classes of signals, all of which can be attributed to different compounds depending on the present conditions.

Experiment 2.3 [Te, CsI, and $B(OH)_3$ in a reducing atmosphere] showed a tellurium signal at the energy 571.8 eV. This was the only time this signal was detected, and it was tentatively attributed to some form of cesium telluride. Depending on the ratio of Cs to Te, the signal varied between 572.4 to 572.7 for the Te-Cs bond.[42] This range of tellurium signals typically includes metal tellurides, and there should be no other metals available in the system (unless the furnace tube itself is corroded, which there was no sign of).

The signals between 576.3 and 576.9 were attributed to TeO_2,[43] and alternatively, TeO_3.[44] The signals for these compounds are close to one another, and determining one from the other with certainty is difficult. There were also a pair of signals at the lower end of this range, at 575.7 eV and 576.0 eV. These signals were

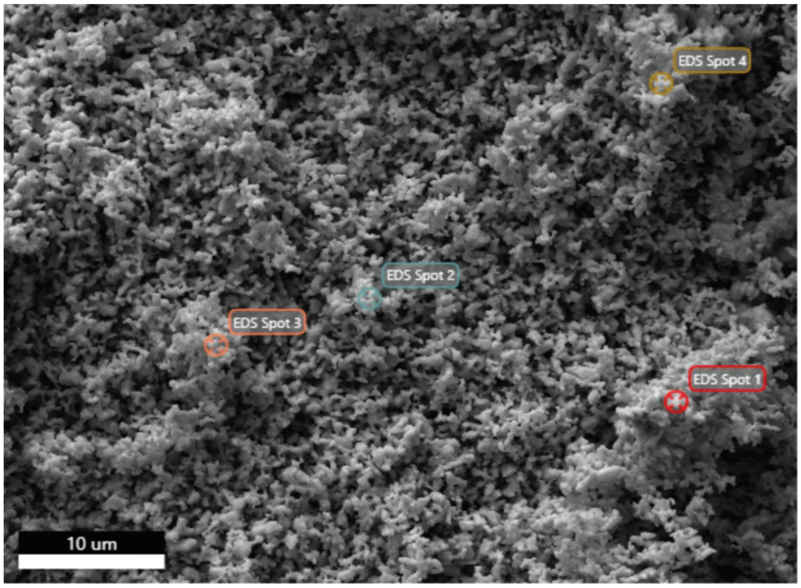

Fig. 9. SEM micrograph of the filter exposed to Te, I, $B(OH)_3$, and inert atmosphere.

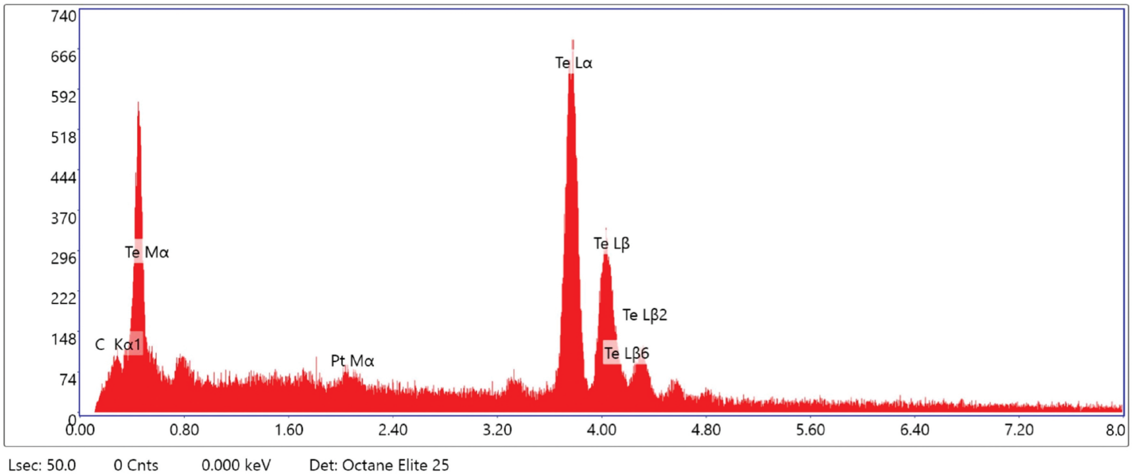

Fig. 10. EDS spectrum of spot 1 in Fig. 9. The filter surface is mostly covered in a porous material that is composed of tellurium.

comparatively low for tellurium oxides, though not unreasonable.[45] They were tentatively assumed to be TeO_2.

Finally, the high-energy signal in experiment 1.1 (oxidizing condition, I, and Te) at 577.9 eV was higher than both TeO_2 and TeO_3. This signal was beyond what tellurium compounds should show in XPS, and no conclusive answer could be given about its nature. It was tentatively assumed to indicate $Te(OH)_6$, a hydrated form of TeO_3 which should have a slightly increased energy compared to the nonhydrated form. However, its energy should be closer to 577 than 578.[45] An example of spectra (survey spectra and detailed spectra of tellurium and iodine) for the oxidizing conditions can be seen in Fig. 11. Notice that the ratio of tellurium to oxygen is slightly above 1:2, implying mostly TeO_2 with some TeO_3.

Finally, for the signals between 573.5 and 574.0, there were two plausible species with similar signals. By comparing the values to literature, this could be metallic tellurium, as the values match well at 573.54 eV[43] and 572.9 eV[44], respectively. The alternative is that these signals were due to tellurium iodide. To investigate this possibility, a sample of tellurium iodide was prepared inhouse and measured with powder X-ray-diffraction (PXRD). The resulting spectrum for the compound can be seen in Fig. 12. It matched well with the reference spectrum, TeI_4 (blue peaks), though some contaminants seemed to be present as well. Most likely this was due to a different

TABLE IV

Peak XPS Signal Position for Each Element and Each Experimental Condition

Experiment	Tellurium Signal Peak, $3d_{5/2}$ (eV)	Iodine Signal Peak, $3d_{5/2}$ (eV)	Cesium Signal Peak, $3d_{5/2}$ (eV)
1.1	576.4	618.9	–
	577.9	620.3	
2.1	576.5	619.2	–
3.1	573.8	618.6	–
	576.8	619.9	
1.2	576.4	618.8	–
		620.1	
2.2	574.0	619.5	–
3.2	573.7	619.5	–
1.3	575.7	618.3	723.9
	576.9	619.6	725.3
2.3	571.8	617.5	723.2
	573.5	619.0	724.7
	576.0	620.1	
3.3	573.6	619.4	725.2
	576.5	620.5	–

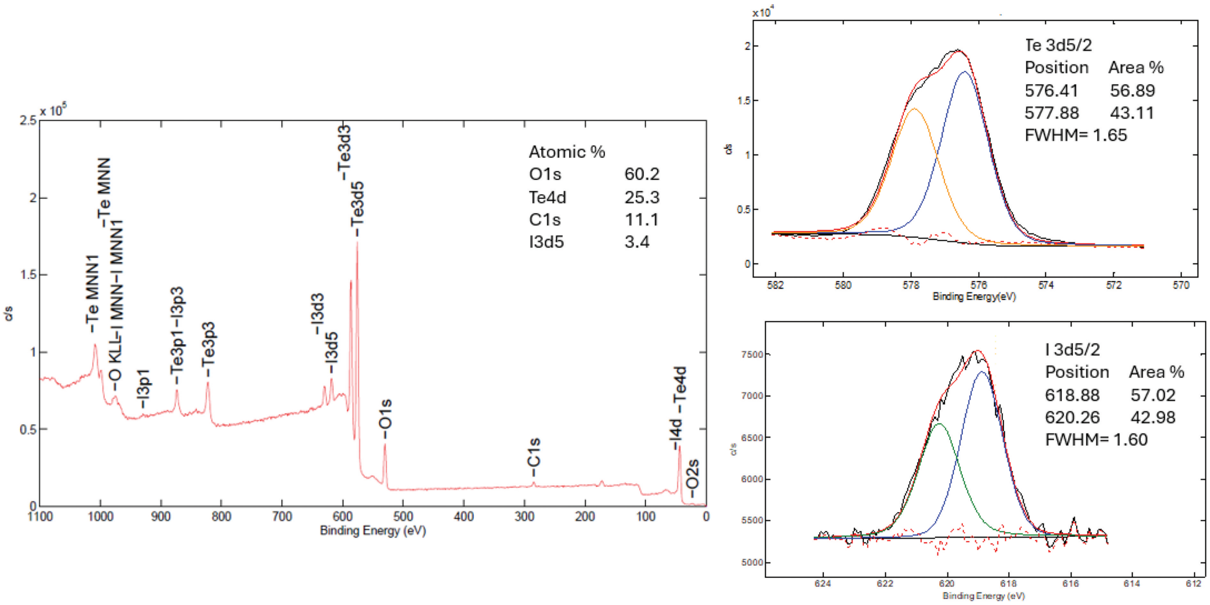

Fig. 11. Survey spectrum and elemental abundance of the filter exposed to oxidizing conditions and Te and I. Also, the spectrum for the (top) tellurium and (bottom) iodine.

stoichiometry of tellurium and iodine in different parts of the sample (potentially Te-I). As the sample was formed as a solid lump, the iodine and tellurium ratio varied with location during formation.

This sample was measured with XPS. However, the elemental composition revealed the ratio of tellurium to iodine being almost 4:1. Likely this was due to the synthesis method. As the tellurium iodide was formed as a solid lump, the ratio of elements could be expected to vary between different parts of the solid. The resulting spectrum for that sample can be seen in Fig. 13. The compound gave a tellurium signal at 573.7 eV, matching very well with the signals at 573.5 to 574 eV.

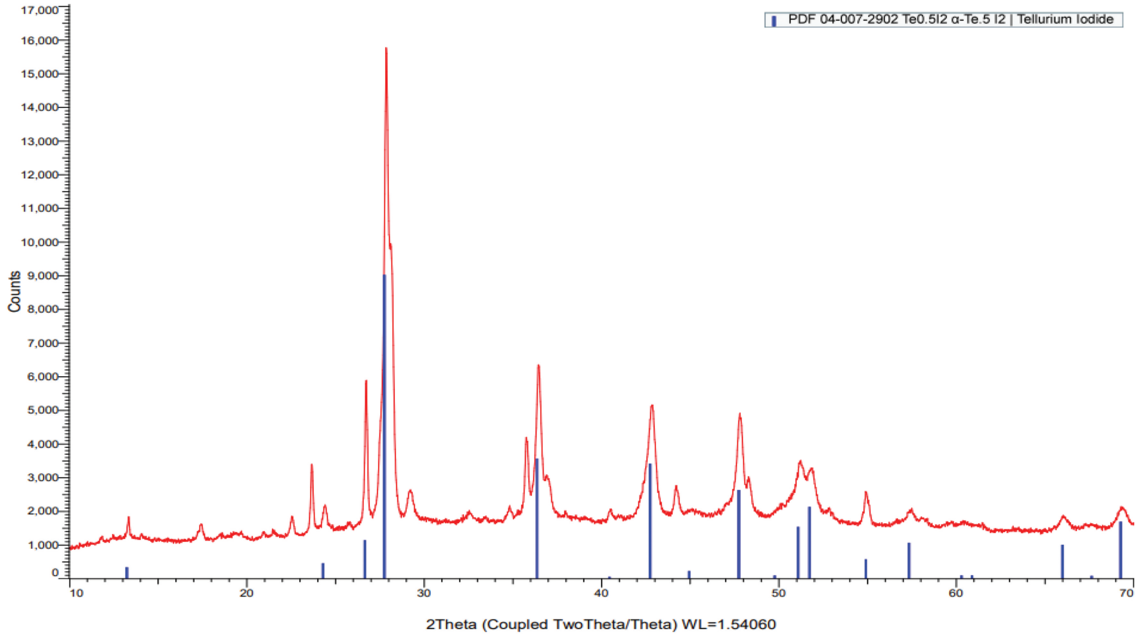

Fig. 12. PXRD of the inhouse-produced sample for tellurium iodide (red line). The blue lines indicate the reference spectrum TeI_4.

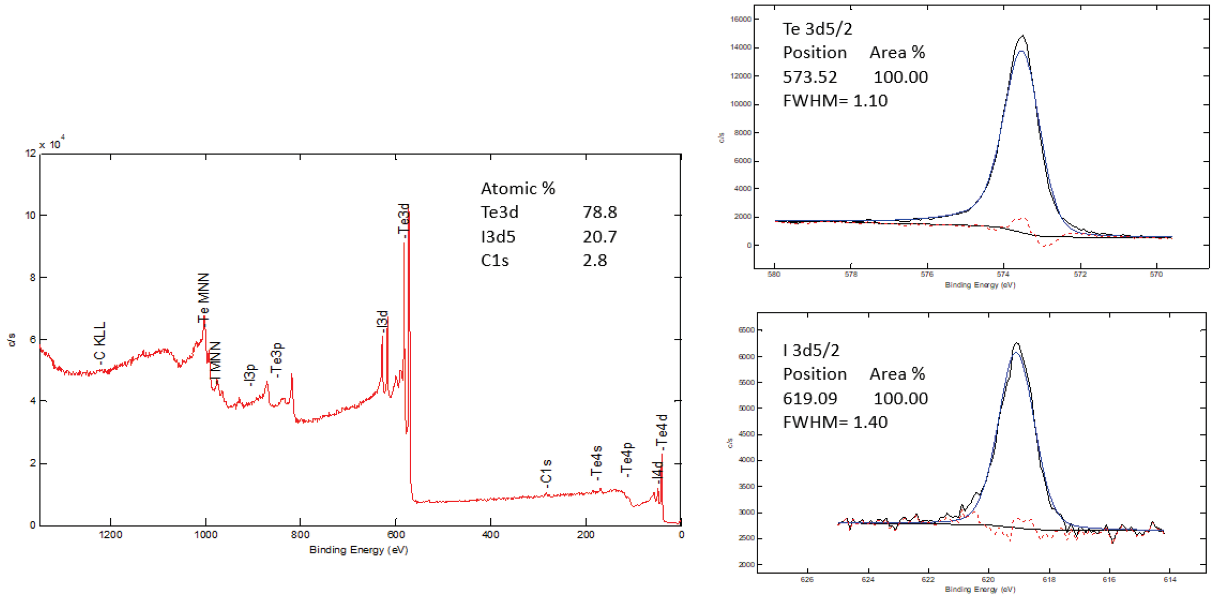

Fig. 13. Survey spectrum and elemental abundance of the Te_4I prepared inhouse. Also, the spectrum for the (top) tellurium and (bottom) iodine.

Based on these results, the hypothesis that tellurium iodide can be difficult to differentiate from tellurium metal is strengthened. Clearly, if the iodine content is relatively low, the XPS signals will overlap. However, as tellurium iodide was confirmed in the samples using SEM-EDS, and could also be implied from XPS, it appears that this compound had formed.

The survey spectra, and the relevant spectra for iodine and tellurium, are included for the reducing condition in Fig. 14 and for the inert condition in Fig. 15. The survey spectra implied that the behavior of iodine was different in the reducing condition compared to the inert (and oxidizing) case, as the iodine fraction was significantly higher in the reducing case: 31% compared

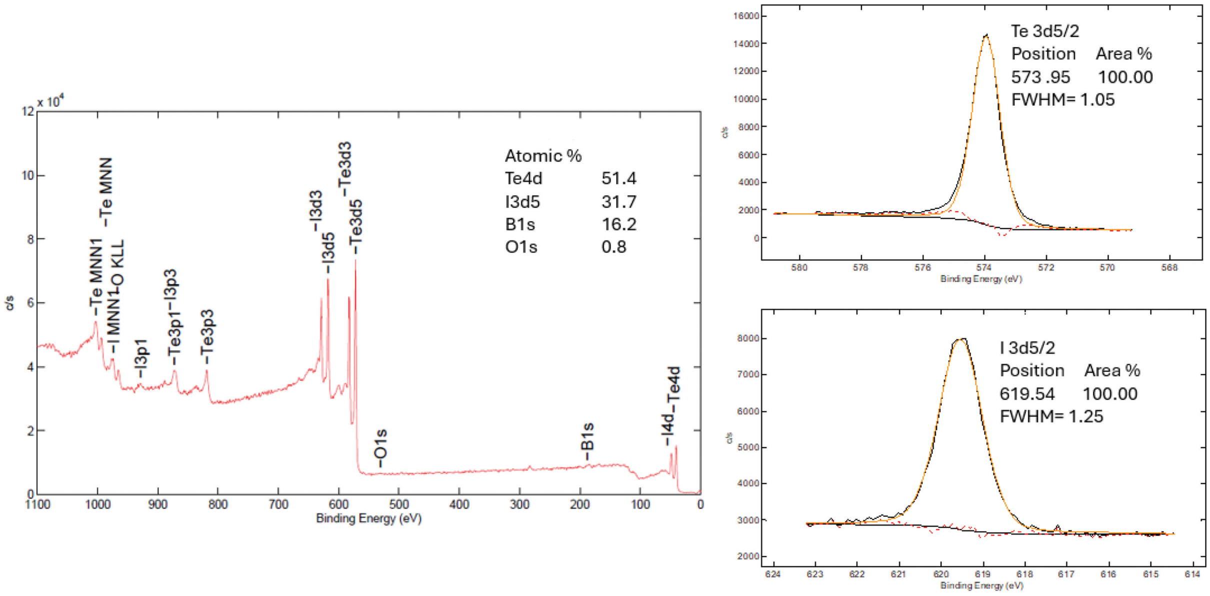

Fig. 14. Survey spectrum and elemental abundance of the filter exposed to reducing conditions and Te, I, and $B(OH)_3$. Also, the spectrum for the (top) tellurium and (bottom) iodine.

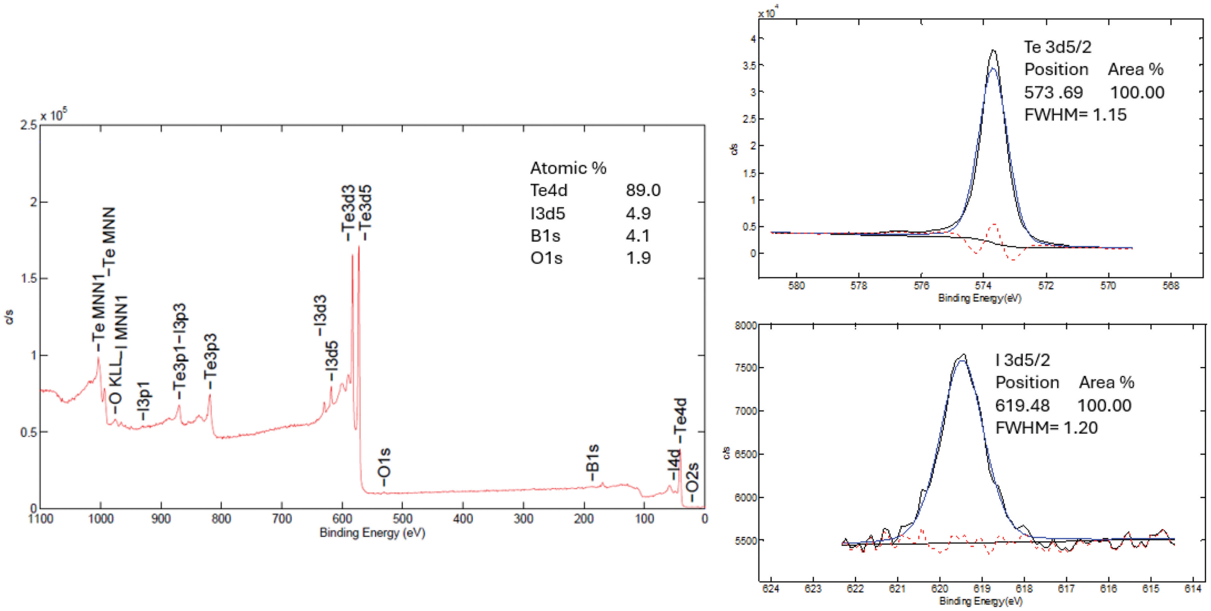

Fig. 15. Survey spectrum and elemental abundance of the filter exposed to inert conditions and Te, I, and $B(OH)_3$. Also the spectrum for the (top) tellurium and (bottom) iodine.

to 4% in the inert case. The oxidizing case (not shown) had an iodine content of 0.7%.

The XPS signals for iodine can roughly be divided into three classes. The most common signal, which was present in almost every sample [except for experiment 1.3, oxidizing atmosphere, with Te, CsI, and $B(OH)_3$ present], varied between the energies of 618.6 to 619.5 eV. The tellurium iodide prepared inhouse displayed an iodine signal of 619.1 eV, matching well. However, it did overlap to some degree with the expected signal for I_2, which ought to have a signal at 619.9.[45] It is possible that both species were present for different experimental conditions. From the survey scans, tellurium iodide may be the reason for the high iodine content in the reducing case with Te, I, and $B(OH)_3$, as seen in Fig. 14. According to the literature,[36] tellurium iodide would not be stable at 650°C, but may form as the temperature falls and be collected on the filter.

The fact that the detailed XPS scans in Figs. 14 and 15 imply the same compounds for tellurium and iodine in both the inert and reducing conditions is worth discussing. As the amount of iodine in the inert case was very low, most of the tellurium would be in the form of tellurium metal in that case. As has been noted, tellurium iodide and tellurium metal are similar in XPS.

The experiments involving cesium iodide in both the reducing and oxidizing conditions each displayed a relatively low signal at 617.5 eV and 618.3 eV, respectively. These signals were assumed to correspond to CsI,[46] though they are slightly low compared to the literature. Several samples also displayed signals around 619.6 eV up to 620.3 eV, which corresponds reasonably well to I_2.

Finally, cesium displays two classes of signals, 723.2 to 723.9 eV and 724.7 to 725.3 eV. For the second range, a certain answer is not possible with XPS alone, as there are two possibilities. As suggested previously, some form of cesium telluride would fit the signal, as its reported value is around 524.6 to 526.4 eV,[42] again depending on the Cs-Te ratio. Lower amounts of Cs give rise to lower energy values. The other alternative is CsOH, with an energy at 724.5 eV.[47]

The first class of signals was attributed to CsI, matching well with some of the literature values.[48] Note, however, that the reported signal for iodine in this paper differed significantly from the signal reported in Ref. [46] for the same compound.

IV.F. Proposed Mechanism for Tellurium Volatility

Across this paper and in Ref. [24], experiments were undertaken that combine tellurium with water and $B(OH)_3$ (described in Ref. [24]), tellurium with iodine (experiments X.1 in this study), and experiments with tellurium, iodine, $B(OH)_3$, and water (experiments X.2 in this study). Only in the last case was there a significant increase in tellurium concentration in the liquid trap. As such, all these components are necessary for this phenomenon to occur. The same results could be seen in all three atmospheres, across the three individual experiments. This implies both that the mechanism is (in principle) independent of the atmosphere, and that the mechanism is consistent.

The analysis with SEM (see Sec. IV.D) confirmed the presence of tellurium iodide on the filters. These are volatile species that are not stable at temperatures above 600°C,[36] implying their formation downstream from the reaction furnace; that is, in a gas stream containing tellurium and iodine.

The proposed mechanism for the increased tellurium volatility can be summarized as the following. After the tellurium was volatilized in the first furnace, the injection of water and iodine at the junction between the furnaces served to lower the temperature of the gas stream. This caused the volatile tellurium to condense into droplets. If there was iodine present in the system, it would react with tellurium to form tellurium iodides, which are gaseous in these conditions. As the temperature increased in the reaction furnace, these dissociated into gaseous tellurium and I_2. In this hypothesis, iodine served to further disperse tellurium to a gaseous species.

Tellurium may react further with water and/or oxygen to form the relatively volatile $TeO(OH)_2$, as depicted in reaction (1). However, as the increase in volatility in these experiments was not dependent on an oxidizing atmosphere, this is not the whole answer. More likely is that the volatile boron species HBO_2 was involved in enhancing the volatility. No evidence was found of a direct reaction between the tellurium and HBO_2, however, though this may be because such a compound is not stable enough to be detected in the aqueous phase. There was also no reference in the literature to any species containing both boron and tellurium relevant to the present conditions.

V. CONCLUSIONS

In all the experiments involving Te, I_2, and $B(OH)_3$, the results agreed unanimously that the volatility of tellurium is increased significantly compared to the same systems lacking any of the aforementioned species.[24] While only one experiment was conducted in each atmosphere, the fact that the same pattern was observed in all three atmospheres implied that this result was both consistent and that the mechanism was not dependent on the atmospheric conditions. However, further repeats are necessary to quantify the effect and conclusively determine the mechanism. However, it should be related to the combination of tellurium, iodine, and boric acid/water, and the formation of tellurium iodide is hypothesized to play a role in it. Furthermore, since the water vapor causes an increase in volatility in both tellurium oxide and boron oxide(s), this is also thought to play a role. The formation of a volatile boron-tellurium compound is a possibility, but could not be conclusively determined.

The filter weights and the liquid trap chemical contents both indicated that the presence of oxygen served to prevent tellurium volatilization at 650°C due to oxidation of tellurium. The filter weights at this atmosphere were consistently the lowest, and the tellurium content of the liquid traps was also very low if not the lowest for any given result.

From the SEM micrographs, the presence of a tellurium-iodide species was confirmed, and the XPS analysis of an inhouse-produced sample of tellurium iodide also lent credence to this confirmation. Evidently tellurium iodide(s) can form under these conditions.

While the liquid trap analysis revealed an increase in the tellurium and boron concentrations when iodine, tellurium, and boric acid were all present together, there was no significant increase in the iodine concentration. This pattern was true for every investigated atmosphere. The boron increases can be explained by the addition of boric acid in this experiment, though the same increase in boron concentration would then be expected in the CsI-$B(OH)_3$-Te experimental series, which did not occur. Potentially, this could be due to the formation of cesium borates, ($Cs_xB_yO_z$), which has been observed previously in similar systems.[28]

The increase in tellurium volatility observed in this study depended on iodine, tellurium, and boron all being present together, and could be of interest for severe accident analysis. Due to ^{132}Te decaying into ^{132}I (with a half-life of 3.17 days), tellurium and iodine will always be present together in a nuclear accident. The addition of boric acid to such a system days or weeks after the accident may potentially cause volatilization of the tellurium.

The formation of tellurium iodides by themselves is potentially of interest from a nuclear accident standpoint. As is depicted in Fig. 1 and experimentally confirmed in Ref. [38], tellurium iodides are more volatile than elemental tellurium and less volatile than elemental iodine. In principle, the formation, therefore, affects the source term of both of these elements. However, it is unlikely that tellurium iodide will form to a significant extent in an accident, where cesium iodide is expected to be the prevailing iodine species. As cesium is a much more common element in nuclear fuel than both iodine and tellurium,[49] it is unlikely that there would be a significant amount of unreacted iodine present to interact with tellurium. However, as some iodine is continuously produced from the decay of tellurium, their interaction cannot be ruled out entirely.

Acknowledgments

The authors acknowledge the CMAL for assistance with PXRD and SEM. Special thanks also to Eric Tam for his assistance with the XPS analysis and to Mark R. StJ. Foreman for his assistance with preparing the TeI_4.

Disclosure Statement

The authors declare that they have no known competing financial interests or personal relationships that could have appeared to influence the work reported in this paper.

Funding

The authors acknowledge the Nordic nuclear safety research organization NKS for partially funding the project.

ORCID

Fredrik Börjesson Sandén http://orcid.org/0009-0005-6571-5650
Anna-Elina Pasi http://orcid.org/0000-0003-4039-3614
Tuula Kajolinna http://orcid.org/0000-0002-8216-1574
Christian Ekberg http://orcid.org/0000-0002-0065-7673

Data Availability

Data will be made available upon reasonable request of the corresponding author.

References

1. J. M. BROUGHTON et al., “A Scenario of the Three Mile Island Unit 2 Accident,” *Nucl. Technol.*, **87**, *1*, 34 (1989); DOI: https://doi.org/10.13182/NT89-A27637.

2. T. HASTE et al., “MELCOR/MACCS Simulation of the TMI-2 Severe Accident and Initial Recovery Phases, Off-Site Fission Product Release and Consequences,” *Nucl. Eng. Des.*, **236**, *10*, 1099 (2006); https://doi.org/10.1016/j.nucengdes.2005.11.012.

3. L. DEVELL et al., “Initial Observations of Fallout from the Reactor Accident at Chernobyl,” *Nature*, **321**, *6067*, 192 (1986); https://doi.org/10.1038/321192a0.

4. V. SAENKO et al., “The Chernobyl Accident and Its Consequences,” *Clin. Oncol.*, **23**, *4*, 234 (2011); https://doi.org/10.1016/j.clon.2011.01.502.

5. K. HIROSE, "2011 Fukushima Dai-ichi Nuclear Power Plant Accident: Summary of Regional Radioactive Deposition Monitoring Results," *J. Environ. Radioact.*, **111**, 13 (2012); https://doi.org/10.1016/j.jenvrad.2011.09.003.
6. A. HASEGAWA et al., "Health Effects of Radiation and Other Health Problems in the Aftermath of Nuclear Accidents, with an Emphasis on Fukushima," *The Lancet*, **386**, *9992*, 479 (2015); https://doi.org/10.1016/S0140-6736(15)61106-0.
7. G. BRILLANT, C. MACHETTO, and W. PLUMECOCQ, "Fission Product Release from Nuclear Fuel I. Physical Modelling in the ASTEC Code," *Ann. Nucl. Ener.*, **61**, 88 (2013); https://doi.org/10.1016/j.anucene.2013.03.022.
8. E. D. V.KAZAKOV, L. ASTAKHOVA, and L. N. ASTAKHOVA, "Thyroid Cancer After Chernobyl," *Nature*, **359**, *6390*, 21 (1992); https://doi.org/10.1038/359021a0.
9. N. KINOSHITA et al., "Assessment of Individual Radionuclide Distributions from the Fukushima Nuclear Accident Covering central-east Japan," *Proc. National Academy of Sciences of the United States of America*, **108**, *49*, 19526 (2011); https://www.jstor.org/stable/23059527 (accessed Jan. 20. 2025).
10. G. STEINHAUSER, A. BRANDL, and T. E. JOHNSON, "Comparison of the Chernobyl and Fukushima Nuclear Accidents: A Review of the Environmental Impacts," *Sci. Total Environ.*, **470–471**, 800 (2014); https://doi.org/10.1016/j.scitotenv.2013.10.029.
11. A.-C. GRÉGORIE and T. HASTE, "Material Release from the Bundle in PHÉBUS FP," *Ann. Nucl. Energy*, **61**, 63 (2013); https://doi.org/10.1016/j.anucene.2013.02.037.
12. T. HASTE, F. PAYOT, and P. D. W. BOTTOMLEY, "Transport and Deposition in the PHÉBUS FP Circuit," *Ann. Nucl. Energy*, **61**, 102 (2013); https://doi.org/10.1016/j.anucene.2012.10.032.
13. A. P. MALINAUSKAS, J. W. GOOCH JR, and J. D. REDMAN, "The Interaction of Tellurium Dioxide and Water Vapor," *Nucl. Appl. Technol.*, **8**, *1*, 52 (1970); https://doi.org/10.13182/NT70-A28633.
14. "1988 Report to the General Assembly, with Annexes—Annex D, Exposures from the Chernobyl Accident," United Nations Scientific Committee in the Effects of Atomic Radiation (1988).
15. J. MAGILL, G. PFENNIG, and Z. S. R.DREHER, *Karlsruher Nuklidkarte—Chart of the Nuclides*, 9th ed., Nucleonica GmbH (2015).
16. "UNSCEAR 2000 Report to the General Assembly, with Scientific Annexes—Volume II: Effects, Annex J: Exposures and Effects of the Chernobyl Accident," United Nations Scientific Committee on the Effects of Atomic Radiation (2000).
17. R. A. LORENZ, E. C. BREHAM, and R. P. WICHNER, "Review of Tellurium Release Rates from LWR Fuel Elements Under Accident Conditions," Oak Ridge National Laboratory (Dec.1983); https://www.osti.gov/servlets/purl/5444891 (accessed Jan. 20, 2025).
18. A. E. PASI, M. RS-J. FOREMAN, and C. EKBERG, "Organic Telluride Formation from Paint Solvents Under Gamma Irradiation," *Nucl. Technol.*, **208**, *11*, 1734 (Nov. 2022); https://doi.org/10.1080/00295450.2022.2061258.
19. A.-E. PASI et al., "Gas Phase Interactions Between Tellurium and Organic Material in Severe Nuclear Accident Scenarios," *Ann. Nucl. Energy*, **197**, 110247 (Dec. 2024); https://doi.org/10.1016/j.anucene.2023.110247.
20. A. E. PASI et al., "Tellurium Behavior in the Containment Sump: Dissolution, Redox, and Radiolysis Effects," *Nucl. Technol.*, **207**, *2*, 217 (Oct. 2021); https://doi.org/10.1080/00295450.2020.1762456.
21. B. SIMONDI-TEISSEIRE et al., "Iodine Behaviour in the Containment of the Phebus FP Tests," *Ann. Nucl. Energy*, **61**, 157 (2013); https://doi.org/10.1016/j.anucene.2013.02.039.
22. Y. PONTILLON, G. DUCROS, and P. P. MALGOUYRES, "Behaviour of Fission Products Under Severe PWR Accident Conditions VERCORS Experimental Programme—Part 1: General Description of the Programme," *Nucl. Eng. Des.*, **240**, *7*, 1843 (2010); https://doi.org/10.1016/j.nucengdes.2009.06.028.
23. Y. PONTILLON and G. DUCROS, "Behaviour of Fission Products Under Severe PWR Accident Conditions—The VERCORS Experimental Programme—Part 2: Release and Transport of Fission Gases and Volatile Fission Products," *Nucl. Eng. Des.*, **240**, *7*, 1853 (2010); https://doi.org/10.1016/j.nucengdes.2009.06.024.
24. F. BÖRJESSON SANDÉN et al., "Effects of Boric Acid on Volatile Tellurium in Severe Accident Conditions," *Annals Nuc. Ener.*, **200**, 110412 (2024); https://doi.org/10.1016/j.anucene.2024.110412.
25. K. H. NEEB, *The Radiochemistry of Nuclear Power Plants with Light Water Reactors*, pp. 27–42, Walter de Gruyter (1997).
26. T. J. CONNOLLY, *Foundations of Nuclear Engineering*, pp. 207–292, John Wiley & Sons Inc. (1978).
27. G. KAUR et al., "Reaction Kinetics During Non-isothermal Solid-State Synthesis of Boron Trioxide via Boric Acid Dehydration, Reaction Kinetiks," *Mechanisms and Catalysis*, **134**, *1*, 347 (2021); https://doi.org/10.1007/s11144-021-02084-8.
28. M. GOUËLLO et al., "Interaction Between Caesium Iodide Particles and Gaseous Boric Acid in a Flowing System Through a Thermal Gradient Tube (1030K–450 K) and Analysis with ASTEC/SOPHAEROS," *Prog. Nucl.*

Energy, **138**, 103818 (2021); https://doi.org/10.1016/j.pnucene.2021.103818.

29. J. L. MARGRAVE, "Gaseous Molecules of Geochemical Significance," *J. Phys. Chem.*, **60**, 6 (1956); https://doi.org/10.1021/j150540a003.
30. L. SOFFER et al., "Accident Source Terms for Light-Water Nuclear Power Plants—Final Report," Office of Nuclear Regulatory Research, U.S. Nuclear Regulatory Commission (1995).
31. M. GOUËLLO, J. HOKKINEN, and T. KÄRKELÄ, "Advances in the Understanding of Molybdenum Effect on Iodine and Caesium Reactivity in Condensed Phase in the Primary Circuit in Nuclear Severe Accident Conditions," *Nucl. Eng. Technol.*, **52**, *8*, 1638 (2020); https://doi.org/10.1016/j.net.2020.01.029.
32. S. SUNDER, "The Relationship Between Molybdenum Oxidation State and Iodine Volatility in Nuclear Fuel," *Nucl. Technol.*, **144**, *2*, 259 (May 2003); https://doi.org/10.13182/NT03-A3443.
33. T. S. KRESS et al., "Fission Product Transport Behaviour," *Nucl. Technol.*, **1010**, *3*, 262 (1993); https://doi.org/10.13182/NT93-A34789.
34. J. MCFARLANE and J. C. LEBLANC, "Fission Product Tellurium and Cesium Telluride Chemistry Revisited," AECL-11333, Atomic Energy of Canada Ltd. (1996).
35. R. S. DICKSON and G. A. GLOWA, "Tellurium Behaviour in the Fukushima Dai-ichi Nuclear Power Plant Accident," *J. Environ. Radioact.*, **204**, 49 (Oct. 2019); https://doi.org/10.1016/j.jenvrad.2019.03.024.
36. R. KNIEP and A. RABENAU, "Subhalides of Tellurium," *Physical and Inorganic Chemistry, Topics in Current Chemistry*, Vol. 111, Springer Berlin, Heidelberg (1983); https://doi.org/10.1007/3-540-12065-3_3.
37. R. KNIEP, A. RABENAU, and H. RAU, "Phase Relationships in the Te-TeI_4 System," *J. Less Common Met.*, **35**, *2*, 325 (1974); https://doi.org/10.1016/0022-5088(74)90244-6.
38. E. KARLSSON et al., "Adsorption Properties of Iodine on Fused Silica Surfaces When Evaporated from Tellurium in Various Atmospheres," *J. Radioanal. & Nucl. Chem*, **326**, *1*, 711 Dec. 21 2023 (2020); https://doi.org/10.1007/s10967-020-07326-y.
39. H. BÜRGER et al., "Phase Equilibrium, Glass-Forming, Properties and Structure of Glasses in the TeO_2-B_2O_3 System," *J. Mater. Sci*, **19**, *2*, 403 (1984); https://doi.org/10.1007/BF00553563.
40. F. A. STEVIE and C. L. DONLEY, "Introduction to X-ray Photoelectron Spectroscopy," *J. Vac. Sci. Technol. A*, **38**, 6 (2020); https://doi.org/10.1016/j.anucene.2024.110412.
41. T. KAIHO, "Inorganic Iodides," *Iodine Chemistry and Applications*, Published by John Wiley & sons Inc. (2014); https://doi.org/10.1002/9781118909911.ch5.
42. L. SORIANO, L. GALAN, and R. RUEDA, "An XPS Study of Cs_2Te Photocathode Materials," *Surf. Interface Anal.*, **16**, *1–12*, 193 (1990); https://doi.org/10.1002/sia.740160138.
43. A. J. RICCO, H. S. WHITE, and H. S. WRIGHTON, "X-ray Photoelectron and Auger Electron Spectroscopic Study of the CdTe Surface Resulting from Various Surface Pretreatments: Correlation of Photoelectrochemical and Capacitance-Potential Behavior with Surface Chemical Composition," *J. Vac. Sci. Technol. A*, **2**, *2*, 1910 (1984); https://doi.org/10.1116/1.572547.
44. W. E. SWARTZ JR, K. J. WYNNE, and D. M. HERCULES, "X-ray Photoelectron Spectroscopic Investigation of Group VI-A Elements," *Anal. Chem.*, **43**, *13*, 1884 (1971); https://doi.org/10.1021/ac60307a044.
45. J. F. MOULDER et al., *Handbook of X-ray Photoelectron Spectroscopy*," p. 130–131, Perkin-Elmer Corporation (1995).
46. P. M. A. SHERWOOD, "X-ray Photoelectron Spectroscopic Studies of Some Iodine Compounds," *J. Chem. Soc. Faraday Trans. 2: Molecular and Chemical Physics*, **72**, 1805 (1976); https://doi.org/10.1039/F29767201805.
47. H. MORES et al., "XPS Study of Iodine Released in Core Melting Experiments," *Surf. Interface Anal.*, **7**, *1*, 22 (1985); https://doi.org/10.1002/sia.740070106.
48. W. E. MORGAN, J. R. van WAZER, and W. J. STEC, "Inner-Orbital Photoelectron Spectroscopy of the Alkali Metal Halides, Perchlorates, Phosphates, and Pyrophosphates," *J. Am. Chem. Soc.*, **95**, *3*, 751 (1973); https://doi.org/10.1021/ja00784a018.
49. A. G. CROFF and C. W. ALEXANDER, "Decay Characteristics of Once-Through LWR and LMFBR Spent Fuels, High-Level Wastes, and Fuel-Assembly Structural Material Wastes," Oak Ridge National Laboratory, Union Carbide Corporation (1980).